Exploring the Impact of Activity-Dependent Stimulation on Neuroanatomy

By

Jimmy Huy Nguyen
B.S., Wichita State University, 2011

Submitted to the graduate degree program in Clinical Research and the Graduate Faculty of the University of Kansas in partial fulfillment of the requirements for the degree of Master of Science.

Chair: Jonathan Mahnken, Ph.D.

Randolph Nudo, Ph.D.

David Guggenmos, Ph.D

Scott Barbay, Ph.D.

Date Defended: 19 April 2017

The thesis committee for Jimmy Huy Nguyen certifies that this is
the approved version of the following thesis:

Exploring the Impact of Activity-Dependent Stimulation on Neuroanatomy

Chair: Jonathan Mahnken, Ph.D.

Date Approved: 11 May 2017

Abstract

Background: Activity-dependent stimulation (ADS) uses recorded neural activity to trigger stimulation of the brain. Open-loop stimulation (OLS) is independent of neural feedback, thus relying on a machine-generated pattern of stimulation. A previous study found that ADS and OLS both promote fine motor control recovery in a rat model of traumatic brain injury in the primary motor cortex. ADS enhanced recovery of motor function compared to OLS. Investigation of the underlying mechanisms driving motor recovery in response to ADS and OLS is needed.

Methods: Six healthy, adult male rats were implanted with recording electrodes in the premotor cortex (PM) and stimulating electrodes in the somatosensory cortex (S1). Three of the rats were treated with ADS; action potentials (spikes) recorded in the premotor cortex triggered stimulation in S1. Three rats were treated with random OLS mimicking the same rate of stimulation as ADS. After 21 days of stimulation, brain tissue was processed for evidence of morphological differences between the two types of stimulation. Immunohistochemistry was used to label sections for synaptophysin, BDNF, GluR1, and GluR2. Densitometry was used for semiquantitative analysis.

Results: As this was a pilot study with a small sample size, analyses were exploratory. Observed synaptophysin and GluR1 immunoreactivity (IR) was greater in ADS rats compared to OLS rats (p=0.0253 and p=0.0253 respectively), whereas BDNF and GluR2 lacked such trends (p=0.456 and p=0.456 respectively). In all rats the stimulated hemispheres expressed significantly more synaptophysin (p= 0.0132) and GluR1 (p=0.0062) than the non-stimulated hemispheres. BDNF and GluR2 expression were significantly lower in the stimulated hemispheres (p=0.0030 and p=0.0054 respectively).

Conclusions: The data suggests that ADS and OLS both enhance synaptogenesis and GluR1 expression. Results are consistent with the hypothesis that ADS induces greater synaptogenesis and GluR1 expression than OLS. Data does not support the hypothesis that BDNF expression is higher after ADS treatment than OLS treatment. This pilot study elucidates the impact of intracortical stimulation on synaptic plasticity in the cerebral cortex.

Acknowledgments

I want to thank my beautiful fiancée (soon to be wife!) for her support throughout the years. She grounds me in reality and keeps me moving forward. The toll of endless days and evenings studying is lightened by the incredible effort she invests in keeping our lives together. I owe everything to her.

Dr. David Guggenmos has my special thanks for guiding me throughout the entire process of experimental design, execution, and analysis. His generosity with his time and his clear minded advice were not only invaluable, but also inspiring.

Dr. Scott Barbay deserves many thanks for helping me throughout the many days of tissue processing and data analysis. Our discussions kept my scientific inquiry headed in the right direction. He provided encouragement and optimism that things would work out. They did.

I want to thank the members of the Nudo lab, including Dr. Heather Hudson, Dr. David Bundy, Dr. Hongyu Zhang, Dr. Kevin Elliott, Dr. Shawn Frost, Max Murphy, Alberto Averna, Caleb Dunham, Jordan Borrell, Stefano Milighetti, and Jean Sunega, for their kind assistance to this first year graduate student. They were always willing to help and open to discussion about issues that arose. Heather especially has my thanks for coming to the rescue when I had problems in the wet lab or with the microscope.

I would like to thank the chair of my thesis committee, Dr. Jonathan Mahnken, for graciously taking on the extra work in his busy schedule.

I want to thank Dr. Nudo allowing me the opportunity to work in his lab. He provided much needed perspective on my experiment and scientific career as a whole. This has been a unique experience that could have only been possible in Dr. Nudo's lab.

Thank you all.

Table of Contents

List of Figures

List of Tables

Introduction

Stroke devastates over 1.6 million people around the world each year (Strong, Mathers, & Bonita, 2007). Half of stroke survivors are burdened with long lasting disabilities. These patients, alongside those impacted by traumatic brain injuries (TBI), currently have few options for rehabilitation. Advances in brain-computer interfaces provide a promising vector for neurorepair and restoration of lost function (Greenwald, Masters, & Thakor, 2016). In this study we examine the effects of a brain-machine-brain interface (BMBI) designed to facilitate motor function recovery after stroke or TBI.

As the name entails, a BMBI first discriminates neural activity from the brain and then processes that information in a machine or prosthesis. The final B in the acronym means that feedback is supplied to the brain, creating a loop of information exchange between brain and machine. Feedback can be partially provided by visual cues or peripheral stimulation, but the BMBI used in this study provides feedback by electrically stimulating the brain through an implanted electrode. When recording and stimulating electrodes are implanted distantly from each other, BMBIs can function as artificial communication links between separate regions of brain. This unique function of BMBIs can be exploited for activity-dependent stimulation (ADS); discriminated action potentials (spikes) are recorded in one brain location and are used to directly trigger stimulation in another brain location. A landmark study by Jackson et al. utilized recording and stimulating electrodes implanted separately in primate primary motor cortex (M1) (Jackson, Mavoori, & Fetz, 2006). Within a couple of days of activity-dependent stimulation, output properties of the recording site began to resemble the output properties of the stimulation site. Augmenting corticocortical interconnections in that way drives specific neurophysiological changes specific to the targeted regions (Jackson et al., 2006).

A relatively new application of BMBIs is to promote brain repair after TBI (Guggenmos et al., 2013). In that study, adult rats received a traumatic brain injury in their primary motor cortex (M1). One group of rats was treated with an ADS protocol that triggered stimulation in the somatosensory cortex (S1) based on spikes recorded in the premotor cortex (PM). The rational was to reestablish connections between S1 and PM, which were attenuated by damage to M1. A second group of rats was treated with random, open-loop stimulation (OLS) in the somatosensory cortex. ADS treated rats recovered fine motor control more quickly than OLS treated rats; while both treatments were superior to non-stimulated control rats. The behavioral recovery was empirically remarkable, however the underlying cellular mechanisms responsible for the effect differences between ADS and OLS remain unclear. Our aim in this study was to elucidate those mechanisms.

In ADS treated rats from the previous study, neural activity in RFA was significantly elevated in the 28-ms following stimulation in S1. Those results suggest that the network interactions between S1 and RFA were reinforced by ADS. A study by Song et al. applied ADS between two sites in primate S1 and also observed strengthened connections between the recording and stimulation site, measured by increased number of matched activity pairs (Song, Kerr, Lytton, & Francis, 2013). The altered network connections observed in these experiments provide evidence that Hebbian synaptic plasticity is involved in the impact of ADS in the neocortex (Guggenmos et al., 2013; Jackson et al., 2006; Song et al., 2013).

One mechanism associated with Hebbian plasticity is long-term potentiation (LTP), which enhances the efficacy of presynaptic neurons in exciting postsynaptic neurons and is central to neocortical plasticity (Foeller & Feldman, 2004). LTP is an example of spike-timing dependent plasticity because its induction depends on temporal relationship between excitatory

postsynaptic potentials (EPSP) and back action potentials (bAP) (Feldman, 2012). Causal relationships, where one neuron consistently fires before the excitation of another neuron, are crucial to LTP induction (Levy & Steward, 1983). This manifests at synapses when EPSPs consistently occur before bAPs. ADS also establishes causal relationships between populations of neurons by stimulating one population of neurons a few milliseconds after detecting spikes in a separate population of neurons (Guggenmos et al., 2013). The similarity between LTP induction criteria and ADS protocols suggests that long-term potentiation (LTP) is a candidate mechanism to explain ADS induced plasticity. Trafficking of AMPA receptors to post-synaptic membranes is crucial to LTP; higher AMPA receptor expression on post-synaptic membranes increases synaptic efficiency at transmitting glutaminergic signals released from pre-synaptic neurons (Aroniadou & Keller, 1995; Huganir & Nicoll, 2013). The AMPA receptor subunit GluR1 is permeable to calcium and rapidly appears on the post-synaptic membrane in LTP. Its presence in the absence of other AMPA receptor subunits is sufficient for LTP (Jia et al., 1996; Kida et al., 2016; Uesaka, Hirai, Maruyama, Ruthazer, & Yamamoto, 2005). Calcium influx is crucial to operating the cellular machinery related to LTP (Feldman, 2012; Huganir & Nicoll, 2013). The insertion of GluR2, a calcium impermeable subunit, occurs at a later phase to stabilize basal synaptic transmission (Meng, Zhang, & Jia, 2003). Changes in AMPA receptor subunit expression would be evidence of modulation of synaptic efficiency and possibly LTP.

Other promising measures to study the structural impact of ADS and OLS are brain-derived neurotrophic factor (BDNF) and synaptophysin. BDNF is a well-documented neurotrophin integral to neural plasticity. Among the wide array of effects promoted by BDNF are synaptogenesis, angiogenesis, and brain remodeling. Expression levels of BDNF vary in response to motor activity and sensory stimuli (Macias et al., 2009; Rocamora, Welker, Pascual,

& Soriano, 1996). AMPA receptor activation can mediate motor recovery after stroke by elevating BDNF levels (Alia et al., 2017; Clarkson et al., 2011; Uesaka, Ruthazer, & Yamamoto, 2006). Reciprocally, BDNF is required for LTP induction (Park & Poo, 2013). Perhaps in part due to BDNF regulation, activities such as motor training and cortical stimulation intensify synaptogenesis (Adkins, Hsu, & Jones, 2008; Kleim et al., 2004). Synaptophysin is a protein located within presynaptic vesicles and is used as a common measure of synaptic density (Stroemer, Kent, & Hulsebosch, 1995). Increases in synaptophysin expression indicate the presence of synaptogenesis.

We aimed to test the hypothesis that ADS will induce neuroplasticity as shown by increases in GluR1, BDNF, and synaptophysin expression. Measuring these markers reveals the nature of changes in local neural circuitry following ADS compared with OLS. Healthy rats were treated with either ADS or OLS in daily sessions conducted for 21 days. Immunohistochemistry was used to label synaptophysin, BDNF, GluR1, and GluR2 in brain sections after 21 days of stimulation. Densitometry was performed for semiquantitative analysis of the immunoreactivity (IR) of each antigen. A secondary aim was to compare the changes in the stimulated hemispheres with the non-stimulated hemispheres using the same semiquantitative analysis as previously mentioned. We hypothesize that intracortical stimulation enhances synaptogenesis, BDNF, and GluR1 expression in the ipsilateral neocortex.

Materials and Methods

Animals

Six adult, male Long Evans rats weighing 350-400g at 4 months old were used in this experiment. The University of Kansas Medical Center Institutional Animal Care and Use Committee approved the protocols for animal use which adhered to the Guide for the Care and Use of Laboratory Animals (National Research Council (U.S.). Committee for the Update of the Guide for the Care and Use of Laboratory Animals., Institute for Laboratory Animal Research (U.S.), & National Academies Press (U.S.), 2011). Animals were assigned to be treated with ADS or OLS as seen in Table 1.

Table 1. Grouping of Rats into Activity-Dependent Stimulation (ADS) or Open Loop Stimulation (OLS).

	ADS	**OLS**
# Rats	3	3
Total	6	

Surgical Procedures

The rats were induced with gaseous isoflurane prior to surgery within a sealed vaporizer chamber. Anesthetization followed with injections of ketamine (80-100 mg/kg IP) and xylazine (5-10 mg/kg). Maintenance boluses of ketamine (10-100 mg/kg/h ip or im) were repeatedly injected as needed throughout the procedure. A stereotaxic frame secured the rat head, and an anal temperature probe was used to monitor the rat's temperature. Rat eyes were protected with ophthalmic ointment. Either Lidocain/Prilocaine cream or bupivacaine were applied to the scalp prior to making a skin incision spanning rostro-caudally between ~6 mm rostral to bregma and ~5 mm distal to the atlanto-occipital junction. The cisterna magna or upper vertebrae were

exposed by reflecting the overlaying neck muscles. The spinal dura located in the foramen magnum was slightly punctured to control brain edema by allowing CSF drainage. After retraction of the temporalis muscle, a craniectomy was performed to expose the primary motor (Caudal Forelimb Area: CFA) and premotor (Rostral Forelimb Area: RFA) cortical areas. Electrophysiological procedures were facilitated by removal of the dura and application of sterile silicone oil to the cortex.

Localization of Cortical Brain Areas

Stimulation and recording areas were localized at S1 and RFA respectively with the intracortical microstimulation (ICMS) technique (Kleim, Barbay, & Nudo, 1998). A tapered glass micropipette with a sharply beveled tip of ~10-25 μm diameter was filled with 3.5 M NaCl and introduced into the cortex. An image of the surface vasculature was taken and displayed on a computer monitor. A fine grid pattern was superimposed over the surface vasculature image, which served as a reference to site the micropipette insertion points. The micropipettes were advanced perpendicular to the cortical surface to a depth of ~1750 μm in order to maximally stimulate the descending pyramidal cells in cortical Layer V. Stimulation pulses composed of 50 ms trains of 200 μs monophasic cathodal pulses delivered at 350 Hz were generated and delivered through the micropipettes. Identification of motor field boundaries was done by observing movements evoked by electrical stimulation up to 80 μA. RFA and CFA were localized with wrist extension, elbow flexion, and occasionally digit movements. Neck and face movement separated RFA and CFA.

Forelimb sensory fields in S1 were identified with multi-unit recordings. A single-shank Michigan style electrode with sixteen recording sites (NeuroNexus, Ann Arbor, MI) was advanced into the sensory cortex to span across cortical layers II-V. Evoked sensory activity was

monitored by playing it through a loudspeaker during the procedure. Further characterization of the spikes was done by amplifying, digitizing, filtering, and displaying on screen (TDT, Alchulta, FL) the recorded neural activity. Electrode penetration sites which responded to palpating the digits, paw and wrist were defined as forelimb sensory fields.

Recording and Stimulation Protocol

A four-shank, sixteen-contact site electrode with 1-1.5 MΩ impedance at each site (A4x4-3mm-100-125-177-CM16LP, NeuroNexus) was chronically implanted into RFA at a maximum depth of 1600 μm. The probe was mated to an active unity gain connector which connected through an amplifier to the recording system (TDT, Alchulta, FL). Neural data could be sorted from the activity of nearby cells in real-time once the neural data acquisition system (TDT, Alchulta, FL) recorded cell activity. A single contact site which detected neural spiking data at a moderate rate of spontaneous activity (4-10 Hz) was selected to be used as the trigger channel for stimulating a cortical site in forelimb-responsive S1.

A second four-shank, sixteen-contact electrode (A4x4-3mm-100-125-177-CM16LP, NeuroNexus) was chronically implanted into S1 and used to stimulate through a single contact with ~200 KΩ impedance. A stimulator isolator and passive headstage (MS16 Stimulus Isolator, TDT) delivered the stimulus. Each neuronal spike recorded from a single contact in RFA triggered a single 60 μA biphasic, cathodal-leading stimulus pulse (200 μs positive 200 μs negative) in S1 after a 10 ms delay. For OLS designated rats, randomized stimuli (Gaussian distribution centered around 7 Hz) were used which approximated the observed frequency in the ADS rats (4-10 Hz). Each stimulus was followed by a 28 ms blanking period to prevent stimulus-activated RFA spikes and stimulus artifact from triggering stimulation.

Both groups were stimulated and recorded daily for 21 days. Daily recording consisted of 80 minute periods of stimulation flanked by 20 minute periods of no stimulation for a cumulative 2 hours if recorded data per day.

Immunohistochemistry Materials

Six primary antibodies were used: polyclonal anti-BDNF antibody (N-20; SC-546) from Santa Cruz Biotechnology, Inc.; monoclonal anti-synaptophysin antibody (MAB5258-I) from Millipore; monoclonal anti-GluR1 antibody (04-855) from Millipore; monoclonal anti-GluR2 antibody (MAB397) from Chemicon; polyclonal anti-GABA A Receptor α1 (06-868) from Millipore; and monoclonal anti-MAP2 antibody (M4403) from Sigma. The six primary antibodies were grouped into three pairs for double immunolabeling, as seen in Table 2. Two secondary antibodies from Molecular Probes, Inc. were used: Goat anti-mouse IgG conjugated with Alexa Fluor 594 and Goat anti-Rabbit IgG conjugated with Alexa Fluor 488. For blocking purposes, 10% normal goat serum (50062Z) was purchased from Life Technologies. VECTASHIELD Mounting Medium with DAPI was acquired from Vector Laboratories Inc. for mounting sections onto slides.

Table 2: Antibody Groupings for Double Immunolabeling

Primary Antibody	Secondary Antibody Fluorophore	Pair	Vendor (number)
Anti-BDNF	Alexa Fluor 488	1	Santa Cruz Biotechnology, Inc (N-20; SC-546)
Anti-Synaptophysin	Alexa Fluor 594	1	Millipore (MAB5258-I)
Anti-GluR1	Alexa Fluor 488	2	Millipore (04-855)
Anti-GluR2	Alexa Fluor 594	2	Chemicon (MAB397)
Anti-GABA A Receptor α1	Alexa Fluor 488	3	Millipore (06-868)
Anti-MAP-2	Alexa Fluor 594	3	Signma (M4403)

Tissue Processing

Within 2 hours following their final recording session, rats were induced with isoflurane within a sealed vaporizer chamber. A lethal dose of Buthanasia (1 cc) was injected ip after induction. Upon cessation of pinch and corneal reflexes, the thorax was quickly opened to facilitate perfusion through the left cardiac ventricle with 350 ml 0.1 M phosphate-buffered saline (PBS) (pH 7.4) followed by 300 ml 4% paraformaldehyde in 0.1 PB (pH 7.4). The brain was removed and post-fixed for 4 hours in 50 ml 4% paraformaldehyde in 0.1 PB (pH 7.4) at 4°C. Cryoprotection was achieved by submerging the brains in 50 ml of 30% sucrose in 0.1 M PB at 4°C for 3-7 days. Non-stimulated hemispheres were marked for easy identification by slicing small cuts into the lateral cortex with a razor blade. A freezing, sliding microtome was used to render 40 μm thick sections ranging from approximately +5.16 mm rostral to bregma to -2.06 mm caudal to bregma. An intermittent region of brain ranging approximately between +2.28 rostral to bregma and -0.24 caudal to bregma was not collected. A reference brain atlas was used

to determine the approximate location of sections based on anatomical features (Paxinos & Watson, 2007). Consecutive sections were collected in well plates containing PBS (pH 7.4).

Double Immunolabeling

As tissue sections were rendered, they were sequentially assigned to be stained with three different primary antibody pairs for double immunolabeling (BDNF/Synaptophysin, GluR1/Glur2, and GABA A Receptor α1/MAP-2) as seen in Table 2. In order, tissues sections would be assigned to pair 1, then pair 2, and then pair 3. Following the assignment of three tissue sections, the next three tissue sections would be discarded, before restarting the sequential assignment to primary antibody pairs. A total of 24-60 sections from each rat were designated for immunohistochemical processing. To reduce non-specific staining, the sections were floated in 5% normal goat serum (NGS) in PBS with 0.3% Triton X-100 for 1 hour. Each tissue section was incubated overnight at 4°C with their two assigned primary antibodies (1:200) (Table 2) and 2% NGS diluted in PBS. Excess primary antibody was rinsed off with three 10 minute washes in PBS before incubation with the two secondary antibodies (1:200) diluted in PBS for 1 hour at room temperature. A final series of three 10 minute washes in PBS cleared off excess secondary antibodies. The sections were mounted onto glass slides with VECTASHIELD mounting medium. Coverslips were sealed with nail polish to prevent leaking of mounting medium.

Image Analysis

The tissue sections were imaged at x200 magnification with a Zeiss Axio Imager.M2 microscope equipped with a Hamamastu ORCA-Flash 4.0 camera. LED light intensity was maintained at 65% on the X-Cite Fluorescence Illuminator. Each section was imaged with three different light channels: DAPI, GFP, and DsRed. Camera exposure time was kept consistent for each respective light channel: 120.060 ms for DAPI, 901.850 ms for GFP, and 1244.959 ms for

DsRed. The microscope was focused using the DAPI light channel in an attempt to maximize the number of cell bodies in focus. Whole section virtual tissues were stitched together using Stereo Investigator (MicroBrightField, Inc. Williston, VT, USA).

Semi-quantitative image analysis was conducted with the Fiji distribution of ImageJ (Schindelin et al., 2012). Within Fiji, single channel virtual tissues were converted to eight-bit gray scale with 0-255 gray levels by changing the image type to 8-bit grayscale. In each section, two separate regions of interest (ROI) were defined in the neocortical areas of the stimulated left hemisphere and the non-stimulated right hemisphere as seen in Figure 1. The ROI medial border was the vertical midline; the ROI deep border was a line drawn perpendicular to the vertical midline and tangential to the most superficial point of the corpus callosum. A third ROI was a polygonal sampling of the corpus callosum, which was sparsely stained tissue. Fiji was used to measure the mean grayscale value of each ROI as a measure of optical density (OD). Relative optical densities (ROD) for both right and left ROIs were calculated (ROD = (OD of target region – OD of corpus callosum)/OD of corpus callosum) (Kang et al., 2013). ROD ratio, defined as the ratio of left hemisphere ROD compared to right hemisphere ROD using a log transformation (ROD ratio = log(Left hemisphere ROD / Right hemisphere ROD). For each individual animal, all of the sections belonging to that respective animal were summed and divided to calculate the mean ROD ratio. The mean ROD ratio was used as the primary measure in the statistical tests.

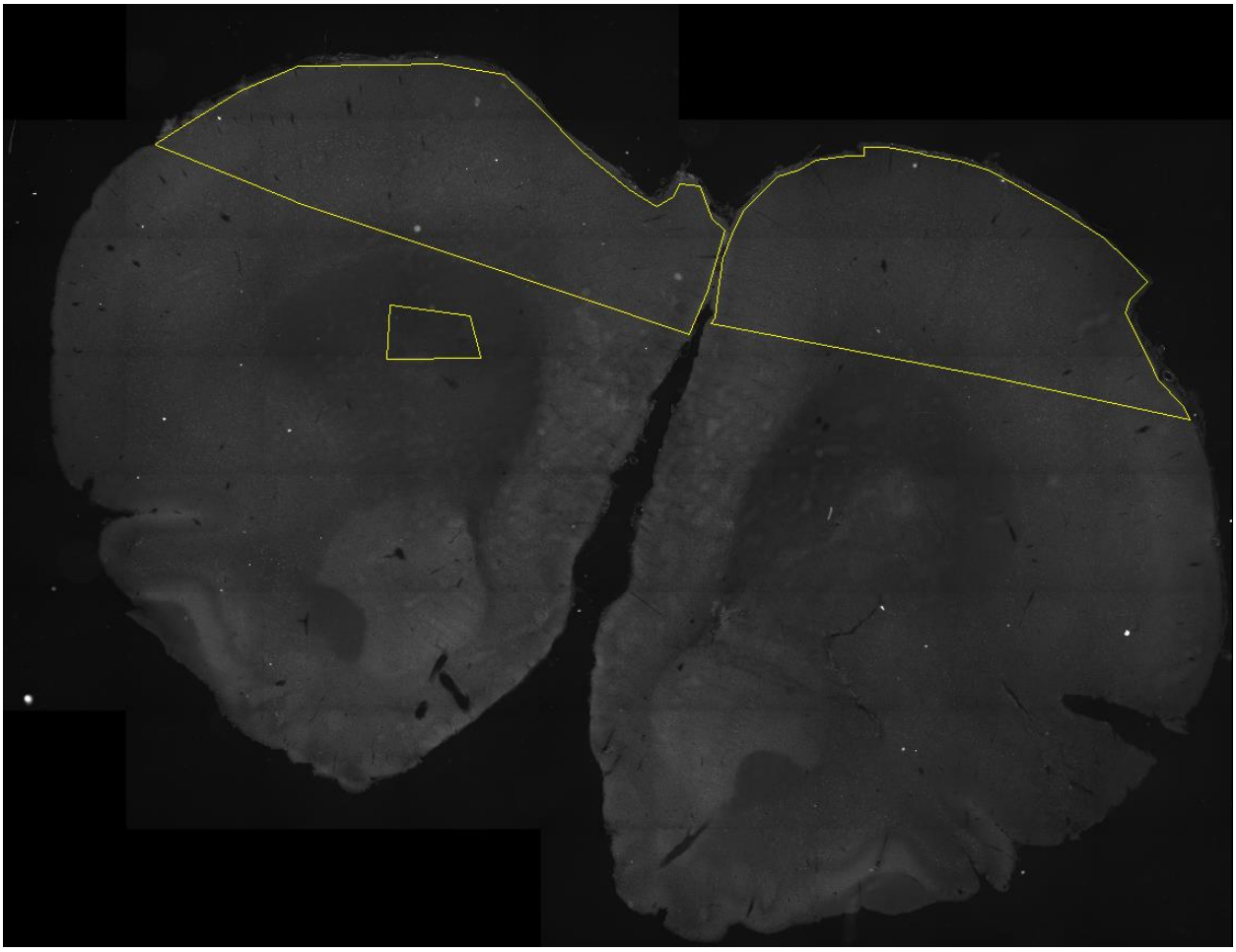

Figure 1: ROI Definitions. This example coronal section is taken from RFA. Regions of interest (ROI) are defined for both the left (stimulated) and right (non-stimulated) sensorimotor cortex. Midline serves as the medial border, and the corpus callosum serves as the deep border. A third ROI is defined within the corpus callosum.

Statistical Analysis

To address the primary aim, ROD ratios of the ADS animals were compared with the OLS animals using a Mood's median test. This test was used to account for the small sample size of three ADS animals compared with three OLS animals. The sample size too small to evaluate the normality assumption required for an ADS vs OLS t test. In the analysis for the secondary aim, mean ROD ratios for each rat were pooled into a single sample. Left hemisphere ROD versus right hemisphere ROD was compared using a single sample Student's t test (two-sided, α

= 0.05, H0: ROD Ratio = 0). Statistical calculations were computed using SAS software, version 9.4 (SAS Institute Inc, Cary, NC, USA).

Results

Specificity of Immunoflourescence

All four antibodies led to diffuse fluorescence throughout the neocortical grey matter. Synaptophysin-like immunoreactivity (IR) was densest around the perimeter of neuronal soma as seen in Figure 2. Co-localization with DAPI confirmed that synaptophysin IR encircles soma with a distinct lack of signal within the cell body itself. BDNF immunolabeling demonstrated mostly cloudy, diffuse signal throughout the neuropil. Discrete elements positive for BDNF IR appear speckled near and possibly within soma. Individual neurons do not necessarily exhibit positive IR for both synaptophysin and BDNF simultaneously; the two markers co-localize inconsistently.

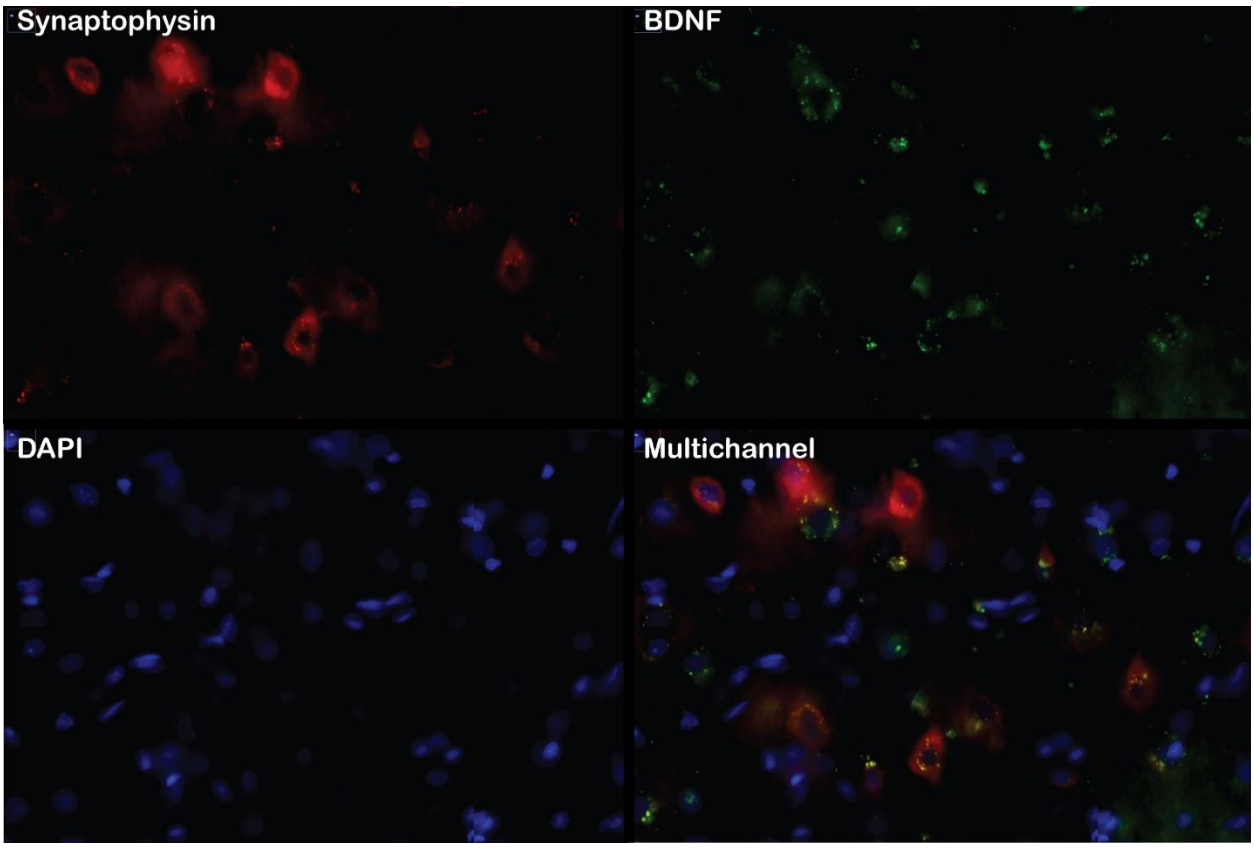

Figure 2: Co-localization of synaptophysin (red) and BDNF (green) immunofluorescence in a double stained section. This image was captured at 400x magnification. DAPI was present in the mounting medium to indicate location of nuclei. Much of the diffuse signal present extracellularly was filtered out of this visualization.

GluR1-like and GluR2-like IR are both concentrated around the perimeter of soma in Figure 3. A higher porportion of neurons are positively stained for GluR2 compared to GluR1. Most GluR1-positive elements appear to be co-localized with GluR2-positive elements. The distribution of GluR2 IR visibly extends onto dendrites, whereas GluR1 IR is more focal around the soma.

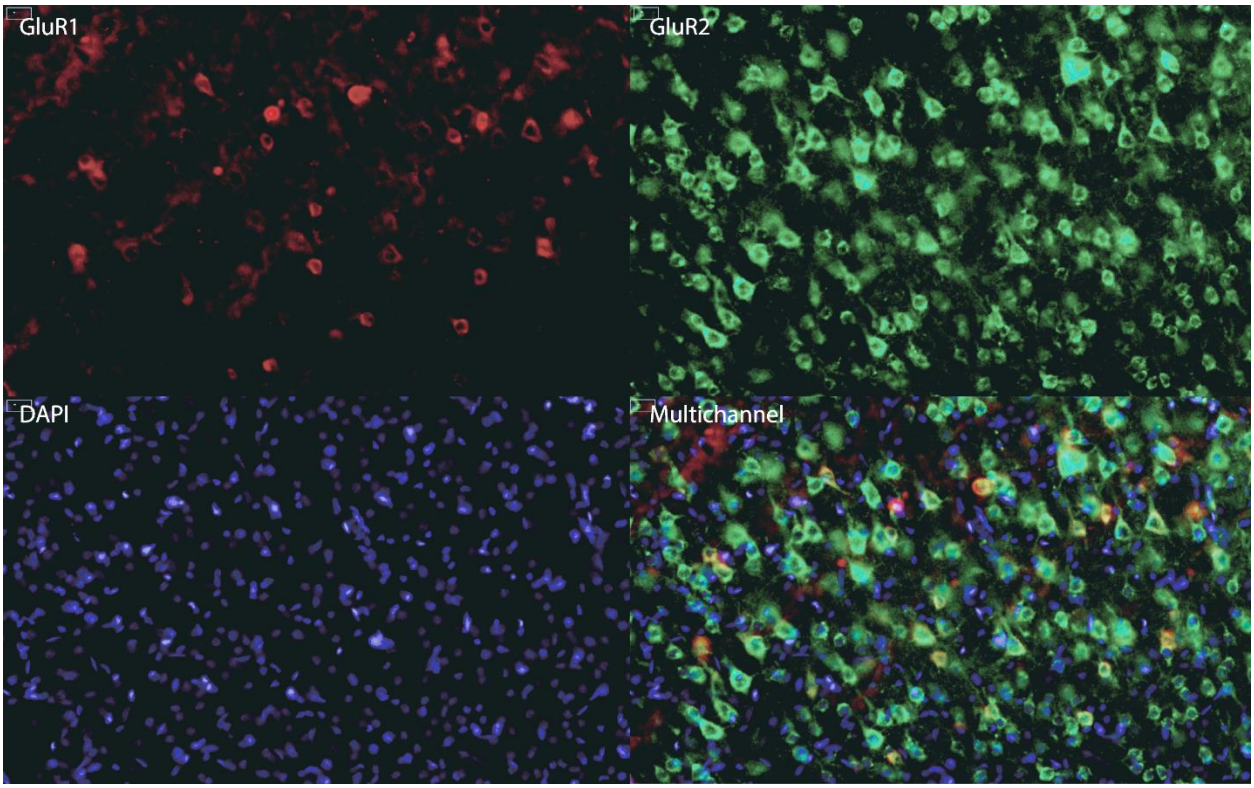

Figure 3: Co-localization of GluR1 (red) and GluR2 (green) within a double stained section. This image was captured at 200x magnification. DAPI was present in the mounting medium to indicate location of nuclei. Much of the diffuse signal present extracellularly was filtered out of this visualization. The color levels were heightened to ease visualization here, however the semi-quantitative data is not affected.

ADS Compared with OLS

For each of the 4 antigens synaptophysin, BDNF, GluR1 and GluR2, 7 to 11 tissue sections per animal were prepared for semi-quantitative analysis. Tissues sections were accepted for semi-quantitative analysis if all three ROIs (left neocortex, right neocortex, and corpus callosum) could be defined within the virtual tissue image. Tissue sections were collected for

GABA A Receptor α1 and MAP-2 immunostaining which will analyzed in a future study. Figure 4 illustrates the mean ROD ratio for each animal. The three highest mean ROD ratio values for both synaptophysin and GluR1 were found in ADS treated animals. Using Mood's median test, the medians of the ROD ratios for synaptophysin and GluR1 were significantly higher in ADS treated animals (p=0.0253 and p=0.0253 respectively). As seen in Figure 4, the differences in expression appear greatest in the S1 region. ADS and OLS animal ROD Ratios are intermixed when ranked from highest to lowest for both BDNF and GluR2. The medians of the ROD ratios for BDNF and GluR2 were not significantly different between ADS and OLS animals (p=0.456 and p=0.456 respectively). Using the current data as reference (mean difference = 0.467, standard deviation = 0.338), a follow-up study powered for a two sample t test comparing synaptophysin ROD ratios in ADS compared with OLS rats would require a total n = 20 rats to achieve 80% power and 5% α. A similar study for GluR1 differences (mean difference = 0.425, standard deviation = 0.167) would require a total n = 8 rats.

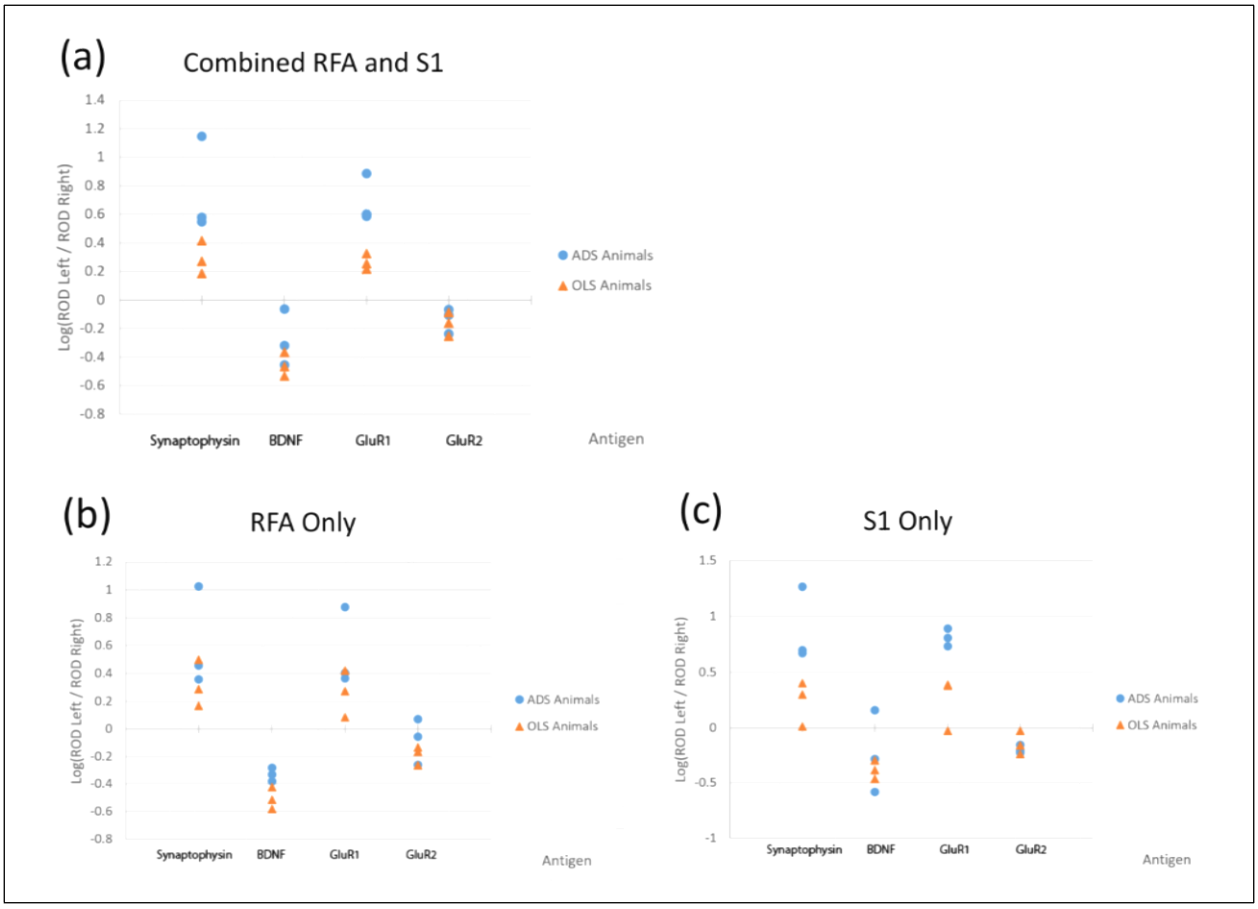

Figure 4: Relative Optical Density (ROD) compared between ADS and OLS animals. (a) The mean ROD ratio for each animal is plotted on the log scale. Synaptophysin and GluR1 ROD ratios were consistently higher in ADS animals than in OLS animals. Less difference is observable with BDNF and GluR2 ROD ratios. (b) The points represent the mean ROD ratios calculated from the subset of RFA derived tissue sections. The differences in expression of synaptophysin and GluR1 do not appear significant in the RFA. (c) The points represent the mean ROD ratios calculated from the subset of S1 derived tissue sections. Much of the differences in synaptophysin and GluR1 expression appear to be focalized in S1.

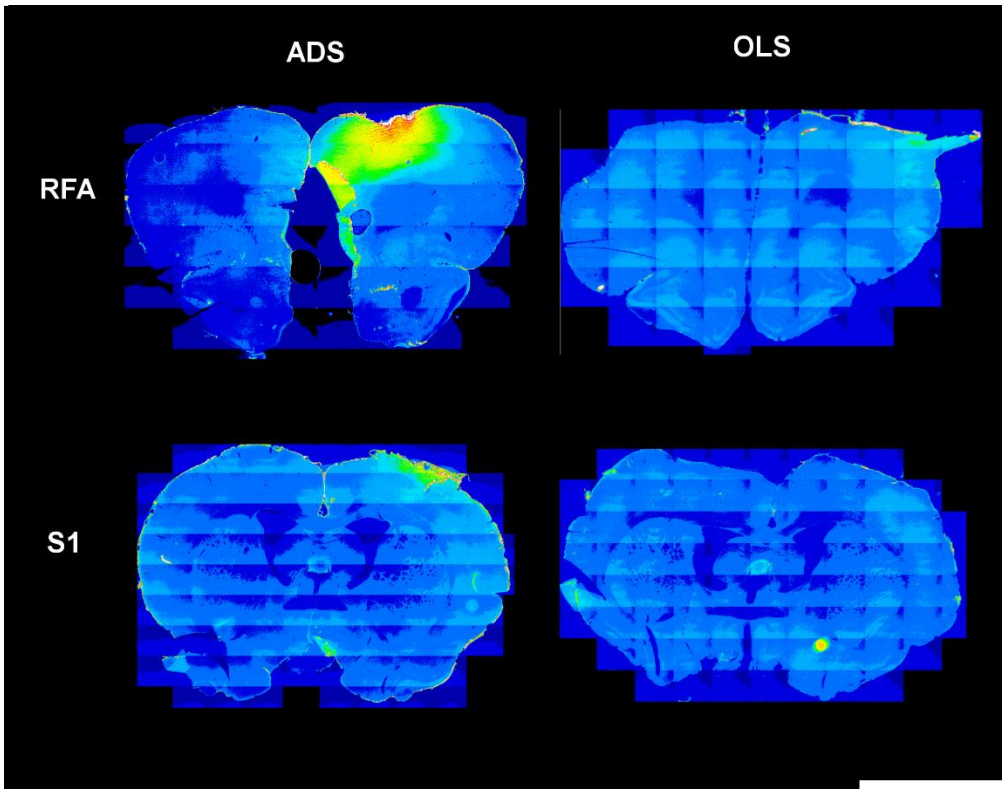

Figure 5: Comparing synaptophysin immunoreactivity between ADS and OLS Animals. These are tissue sections taken from ADS and OLS animals displaying synaptophysin immunoreactivity. The image uses a 16 color look-up table, with red representing the most synaptophysin-specific fluorescence, and black representing no fluorescence. The 16 color look-up table is used only for ease of visualization. Semi-quantitative analyses was done on 8-bit, 255 level images.

Stimulated Hemisphere Compared with Non-stimulated Hemisphere

All six rats were pooled into a single sample to accommodate comparison of IR differences between the stimulated hemispheres (left) and non-stimulated hemispheres (right) as seen in Figure 6. ROD ratios were log transformed before performing t tests to minimize the distortion around 1. Synaphtophysin ROD in the stimulated hemisphere was higher than in the non-stimulated hemisphere ($t(5)=3.76$, $p= 0.0132$). BDNF ROD in the stimulated hemisphere was lower than in the non-stimulated hemisphere ($t(5)=-5.36$, $p=0.0030$). GluR1 ROD in the stimulated hemisphere was higher than in the non-stimulated hemisphere ($t(5)=4.45$, $p=0.0062$). GluR2 ROD in the stimulated hemisphere was lower than in the non-stimulated hemisphere

($t(5)$=-4.69, p=0.0054). As seen in Figure 6, the same general pattern appears in both RFA and S1.

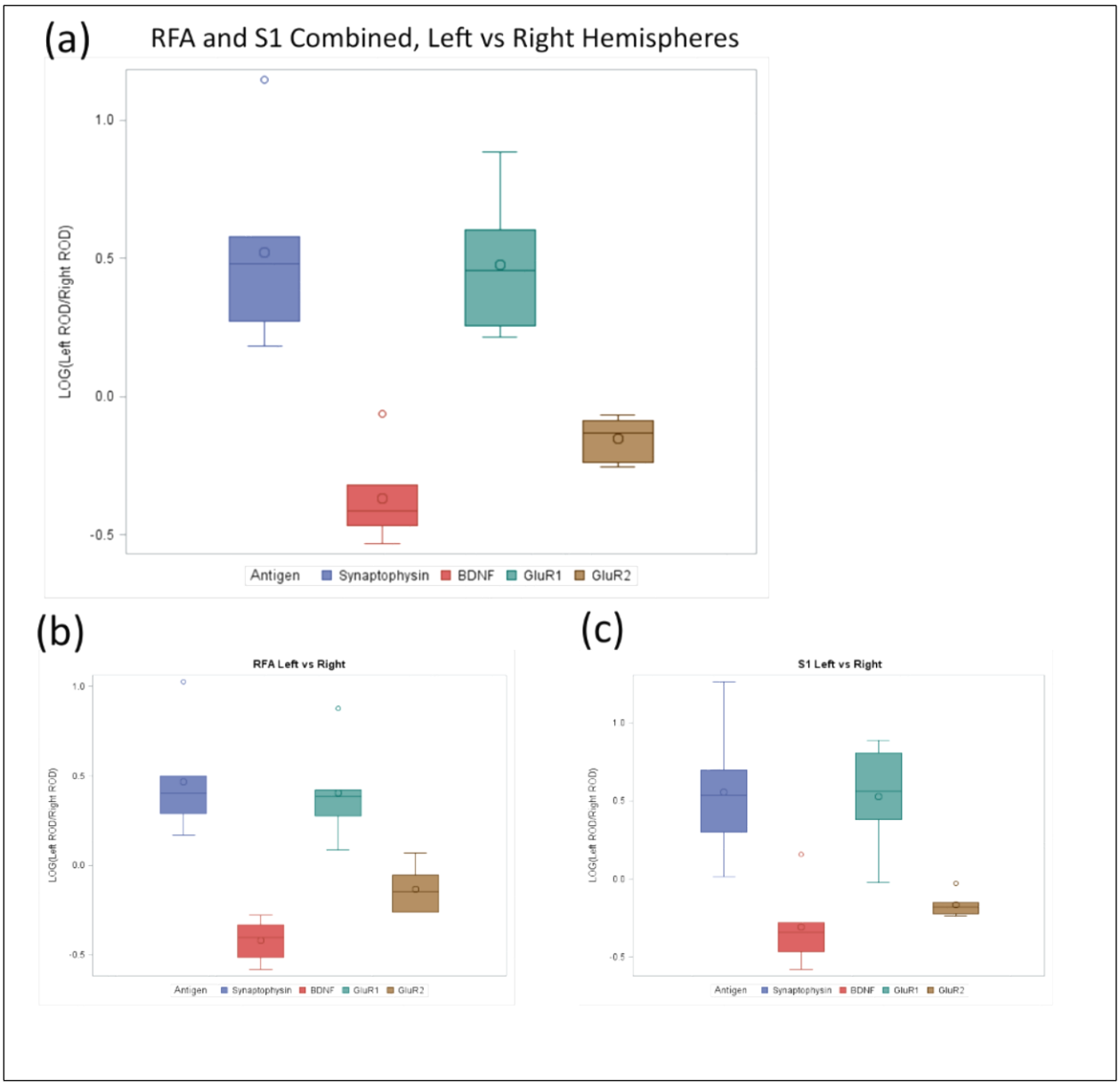

Figure 6: Stimulated hemisphere ROD compared with non-stimulated hemisphere ROD. The left hemisphere is the stimulated hemisphere; the right hemisphere is the non-stimulated hemisphere. All six animals are pooled into a single sample. Log transformed ROD ratios for each animal are plotted. The circles denote means and outliers. (a) The mean ROD ratio accounting for both RFA and S1 is plotted. Synaptophysin and GluR1 expression are both significantly higher on the left (stimulated) hemisphere. BDNF and GluR2 expression are both significantly lower in the stimulated left (stimulated) hemisphere. (b) The mean ROD ratios calculated from the subset tissue sections collected from RFA. (c) The mean ROD ratio calculated from the subset of tissue sections collected from S1.

Correlation between Antigens ROD

Pairs of ROD values calculated from the same section or adjacent sections are plotted on Figure 7 to depict the relationship between synaptophysin, BDNF, and GluR1 IR. Plotting multiple measurements from the same animal violates the independence assumptions required for Pearson's correlation tests. A mixed model approach would be needed to determine the correlation between the different antigens. Qualitatively, there does appear to be a moderate positive correlation between the synaptophysin and BDNF as well as between synaptophysin and GluR1.

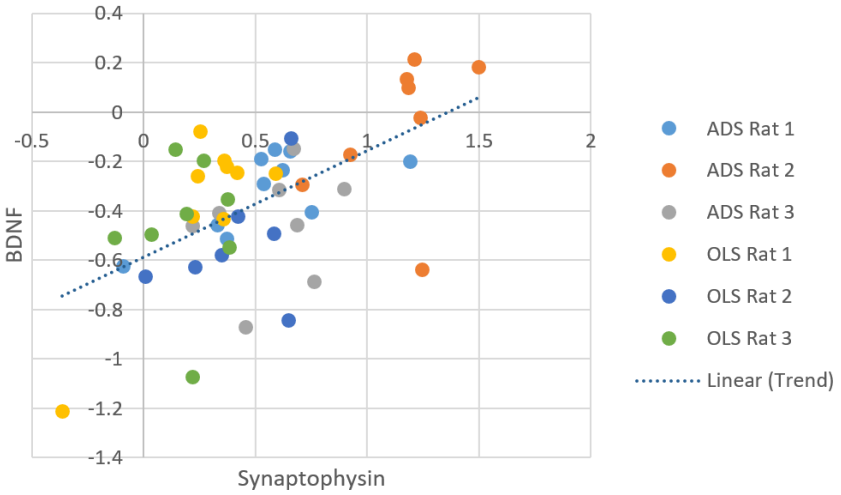

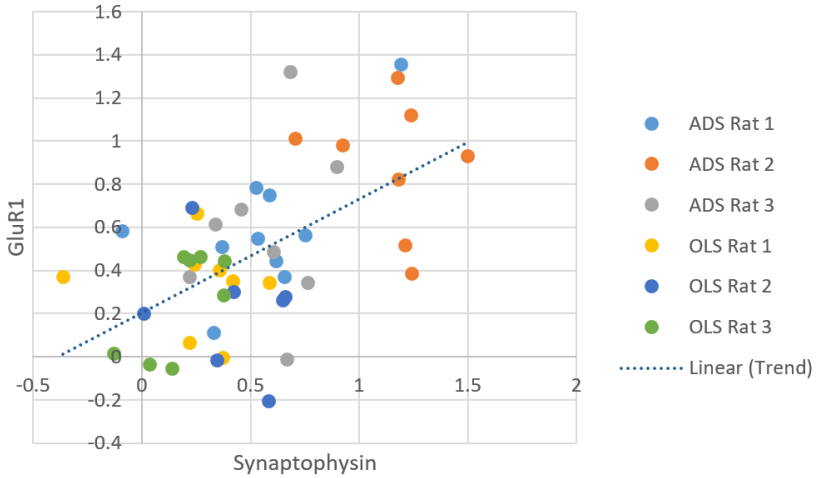

Figure 7: Correlation between levels of synaptophysin, BDNF, and GluR1 ROD. BDNF and synaptophysin were dual-stained together, thus each point represents the paired BDNF and synaptophysin ROD ratio values taken from a single tissue section on the log scale. Synaptophysin and GluR1 were stained on adjacent tissue sections. There appears to be a moderate positive correlation between both sets of antigens.

Discussion

. Addressing the primary research question, there does appear to be a difference in synaptogenesis and GluR1 expression after ADS treatment compared with OLS treatment. For the secondary aim, both ADS and OLS were found to enhance synaptogenesis and GluR1 expression. Findings regarding BDNF were less agreeable with our hypotheses, which is discussed later.

Synaptophysin is a protein present within presynaptic vesicles at nearly all nerve terminals. This quality makes synaptophysin immunoreactivity a useful measure for of approximating the total number of synapses (Stroemer et al., 1995). Relative optical density measurements of synaptophysin in our study are consistent with the secondary hypothesis that intracortical stimulation increases synaptic count in the sensorimotor cortex ipsilateral to stimulation. Adkins et al. found similar increases in synaptic count in sensorimotor cortex following epidural stimulation of the neocortex in an open-loop manner (Adkins et al., 2008). Synaptogenesis also occurs in late phase motor skill learning, thus perhaps it is appropriate to ponder if the neuroplastic response to intracortical stimulation and ADS may be akin to motor skill learning (Guggenmos et al., 2013; Kleim et al., 2004). A novel finding in our study is the observation of synaptic density increases near RFA in response to very distant stimulation in S1. Tracer studies have found sparse corticocortico projections connecting S1 with RFA and M1 (Mohammed & Jain, 2016). The distant changes in RFA may be facilitated by axons extending anterograde from soma located in the stimulated sensory cortex, or the possibility exists that the changes are facilitated by indirect connections via the thalamus.

AMPA receptors with GluR1 subunits are calcium permeable and are inserted into the post-synaptic membrane during the induction of LTP (Aroniadou & Keller, 1995; Huganir &

Nicoll, 2013; Jia et al., 1996). This remains true in the primary motor cortex where GluR1 insertion is integral to the process of motor learning (Hasan et al., 2013; Kida et al., 2016). Plasticity in the somatosensory cortex also relies on the insertion of AMPA receptors (Foeller & Feldman, 2004). The increase of GluR1 expression observed in the present study suggests the involvement of LTP in the cortical response to both ADS and OLS stimulation. A possible positive correlation between GluR1 and synaptophysin ROD increases may indicate a common pathway shared by the two responses to cortical stimulation. The calcium influx following current injection could conceivably co-opt much of the cellular machinery that is associated with LTP, BDNF, or synaptogenesis (Huganir & Nicoll, 2013; Park & Poo, 2013). However the possibility of LTP induction and synaptogenesis existing as completely separate pathways cannot be rejected. Nevertheless, the coincident increases in GluR1 and synaptogenesis ties links between the neural plasticity promoted by cortical stimulation and the process of motor learning.

The data trends towards showing a significant difference between the effects of ADS and OLS on synaptophyin and GluR1 ROD ratio increases. Higher powered studies would be needed to confirm these findings. Such confirmation would inform a mechanistic understanding of the superiority of ADS over OLS at promoting motor recovery after cortical injury (Guggenmos et al., 2013). ADS is hypothetically more suited to inducing spike-timing-dependent plasticity due to the near synchronization between recording and stimulation regions in the brain; increases of synaptogenesis or GluR1 expression following ADS treatment compared with OLS treatment support that hypothesis.

BDNF is a neurotrophin that promotes many processes related to neural plasticity such as synaptogenesis, angiogenesis, and brain remodeling (Park & Poo, 2013). Activity-dependent increases in BDNF expression occur after motor training and peripheral sensory stimulation (Lu,

2003; Macias et al., 2009; Rocamora et al., 1996). Thus the decrease in BDNF IR in the hemisphere ipsilateral to cortical stimulation was an unexpected finding in our study. Such a decrease in conjunction with increased GluR1 IR seemingly conflicts with previous findings of the tightly interdependent relationship between AMPA receptor dependent LTP and BDNF (Clarkson et al., 2011; Park & Poo, 2013); BDNF signaling can be induced downstream of AMPA receptor activation, and the development of LTP is reliant on BDNF. However, previous studies were largely conducted with short-term in vitro organotypic slice cultures or in vivo after lesions with motor training (MacLellan et al., 2011). Perhaps the in vivo chronic stimulation seen here in un-lesioned animals hints at the presence of a yet unconsidered negative feedback mechanism that down-regulates BDNF expression with prolonged intracortical stimulation. One possible actor is that BDNF increases the production of microRNAS (miRNAs) which in turn inhibits the transcription of BDNF to maintain homeostasis (Keifer, Zheng, & Ambigapathy, 2015). It is worth considering whether the diminished BDNF ROD ratios may be due to elevated expression of BDNF in the non-stimulated hemisphere. A contralateral increase in BDNF could account for our decreased BDNF ROD ratios, because we divide the ROD of the stimulated side by the ROD of the non-stimulated side to derive the ROD ratio. However this alternative interpretation also mechanistic explanations and is still not coherent with the hypothesis of BDNF being positively correlated with synaptic changes as measured with synaptophysin and GluR1.

A single rat treated with ADS, labeled as “ADS Rat 2” in Figure 7, developed significantly higher levels of synaptophysin and GluR1 IR than all other rats. Close inspection of the tissue sections collected from ADS Rat 2, as seen on the left side of Figure 5, reveals a small indention into the superficial cortex on the stimulated side which could possibly be unintended

injury or evidence of pressure due to electrode placement. As reviewed by Nudo, brain injury may temporarily suppress growth inhibition and set off a cascade of events enabling neural plasticity (Nudo, 2013). One feasible interpretation is that the presence of injury had a multiplicative effect on the impact of ADS in ADS Rat 2. Similar indentions on the non-stimulated hemisphere of other rats did not result in local increases of IR.

A limitation of the study is the lack of a control group consisting of rats implanted with electrodes but without active stimulation. Such a control group would have allowed discrimination of the effects due purely to the insertion of electrodes, independent of stimulation. Electrodes were always implanted in the left hemisphere; a non-implanted control group would have also allowed exclusion of the possibility that right and left cortical hemispheres naturally express different levels of IR. The present study used the unstimulated cortical hemisphere as the baseline to compare with the stimulated cortical hemisphere, which does not allow us to rule out the possibility of stimulation affecting the contralateral hemisphere. Nevertheless, our methods are conservative because increases of either synaptophysin or GluR1 IR in the contralateral hemisphere would only bias our results towards the null.

Though limited in scope, this study provides valuable insight into the mechanisms underlying synaptic efficacy as demonstrated in the Guggenmos et al. study (i.e., enhanced neural activity in RFA due to ADS stimulation) (Guggenmos et al., 2013). We found that ADS is also associated with enhanced synaptogenesis and mediated through ADS modulation of GluR1 expression. Moreover, the differences in anatomical responses to ADS and OLS are beginning to be revealed. There is clinical significance in learning that ADS and OLS can impact neuroplasticity in the absence of acute brain injury. This perhaps opens the possibility of using ADS or OLS in patients living with disabilities due to previous stroke or TBI.

References

Adkins, D. L., Hsu, J. E., & Jones, T. A. (2008). Motor cortical stimulation promotes synaptic plasticity and behavioral improvements following sensorimotor cortex lesions. *Exp Neurol, 212*(1), 14-28. doi:10.1016/j.expneurol.2008.01.031

Alia, C., Spalletti, C., Lai, S., Panarese, A., Lamola, G., Bertolucci, F., . . . Caleo, M. (2017). Neuroplastic Changes Following Brain Ischemia and their Contribution to Stroke Recovery: Novel Approaches in Neurorehabilitation. *Front Cell Neurosci, 11*, 76. doi:10.3389/fncel.2017.00076

Aroniadou, V. A., & Keller, A. (1995). Mechanisms of LTP induction in rat motor cortex in vitro. *Cereb Cortex, 5*(4), 353-362.

Clarkson, A. N., Overman, J. J., Zhong, S., Mueller, R., Lynch, G., & Carmichael, S. T. (2011). AMPA receptor-induced local brain-derived neurotrophic factor signaling mediates motor recovery after stroke. *J Neurosci, 31*(10), 3766-3775. doi:10.1523/JNEUROSCI.5780-10.2011

Feldman, D. E. (2012). The spike-timing dependence of plasticity. *Neuron, 75*(4), 556-571. doi:10.1016/j.neuron.2012.08.001

Foeller, E., & Feldman, D. E. (2004). Synaptic basis for developmental plasticity in somatosensory cortex. *Curr Opin Neurobiol, 14*(1), 89-95. doi:10.1016/j.conb.2004.01.011

Greenwald, E., Masters, M. R., & Thakor, N. V. (2016). Implantable neurotechnologies: bidirectional neural interfaces--applications and VLSI circuit implementations. *Med Biol Eng Comput, 54*(1), 1-17. doi:10.1007/s11517-015-1429-x

Guggenmos, D. J., Azin, M., Barbay, S., Mahnken, J. D., Dunham, C., Mohseni, P., & Nudo, R. J. (2013). Restoration of function after brain damage using a neural prosthesis. *Proc Natl Acad Sci U S A, 110*(52), 21177-21182. doi:10.1073/pnas.1316885110

Hasan, M. T., Hernandez-Gonzalez, S., Dogbevia, G., Trevino, M., Bertocchi, I., Gruart, A., & Delgado-Garcia, J. M. (2013). Role of motor cortex NMDA receptors in learning-dependent synaptic plasticity of behaving mice. *Nat Commun, 4*, 2258. doi:10.1038/ncomms3258

Huganir, R. L., & Nicoll, R. A. (2013). AMPARs and synaptic plasticity: the last 25 years. *Neuron, 80*(3), 704-717. doi:10.1016/j.neuron.2013.10.025

Jackson, A., Mavoori, J., & Fetz, E. E. (2006). Long-term motor cortex plasticity induced by an electronic neural implant. *Nature, 444*(7115), 56-60. doi:10.1038/nature05226

Jia, Z., Agopyan, N., Miu, P., Xiong, Z., Henderson, J., Gerlai, R., . . . Roder, J. (1996). Enhanced LTP in mice deficient in the AMPA receptor GluR2. *Neuron, 17*(5), 945-956.

Kang, H. H., Wang, C. H., Chen, H. C., Li, I. H., Cheng, C. Y., Liu, R. S., . . . Ma, K. H. (2013). Investigating the effects of noise-induced hearing loss on serotonin transporters in rat brain using 4-[18F]-ADAM/small animal PET. *Neuroimage, 75*, 262-269. doi:10.1016/j.neuroimage.2012.06.049

Keifer, J., Zheng, Z., & Ambigapathy, G. (2015). A MicroRNA-BDNF Negative Feedback Signaling Loop in Brain: Implications for Alzheimer's Disease. *Microrna, 4*(2), 101-108.

Kida, H., Tsuda, Y., Ito, N., Yamamoto, Y., Owada, Y., Kamiya, Y., & Mitsushima, D. (2016). Motor Training Promotes Both Synaptic and Intrinsic Plasticity of Layer II/III Pyramidal Neurons in the Primary Motor Cortex. *Cereb Cortex, 26*(8), 3494-3507. doi:10.1093/cercor/bhw134

Kleim, J. A., Barbay, S., & Nudo, R. J. (1998). Functional reorganization of the rat motor cortex following motor skill learning. *J Neurophysiol, 80*(6), 3321-3325.

Kleim, J. A., Hogg, T. M., VandenBerg, P. M., Cooper, N. R., Bruneau, R., & Remple, M. (2004). Cortical synaptogenesis and motor map reorganization occur during late, but not early, phase of motor skill learning. *J Neurosci, 24*(3), 628-633. doi:10.1523/JNEUROSCI.3440-03.2004

Levy, W. B., & Steward, O. (1983). Temporal contiguity requirements for long-term associative potentiation/depression in the hippocampus. *Neuroscience, 8*(4), 791-797.

Lu, B. (2003). BDNF and activity-dependent synaptic modulation. *Learn Mem, 10*(2), 86-98. doi:10.1101/lm.54603

Macias, M., Nowicka, D., Czupryn, A., Sulejczak, D., Skup, M., Skangiel-Kramska, J., & Czarkowska-Bauch, J. (2009). Exercise-induced motor improvement after complete spinal cord transection and its relation to expression of brain-derived neurotrophic factor and presynaptic markers. *BMC Neurosci, 10*, 144. doi:10.1186/1471-2202-10-144

MacLellan, C. L., Keough, M. B., Granter-Button, S., Chernenko, G. A., Butt, S., & Corbett, D. (2011). A critical threshold of rehabilitation involving brain-derived neurotrophic factor is required for poststroke recovery. *Neurorehabil Neural Repair, 25*(8), 740-748. doi:10.1177/1545968311407517

Meng, Y., Zhang, Y., & Jia, Z. (2003). Synaptic transmission and plasticity in the absence of AMPA glutamate receptor GluR2 and GluR3. *Neuron, 39*(1), 163-176.

Mohammed, H., & Jain, N. (2016). Ipsilateral cortical inputs to the rostral and caudal motor areas in rats. *J Comp Neurol, 524*(15), 3104-3123. doi:10.1002/cne.24011

National Research Council (U.S.). Committee for the Update of the Guide for the Care and Use of Laboratory Animals., Institute for Laboratory Animal Research (U.S.), & National Academies Press (U.S.). (2011). *Guide for the care and use of laboratory animals* (pp. xxv, 220 p). Retrieved from http://www.ncbi.nlm.nih.gov/books/NBK54050

Nudo, R. J. (2013). Recovery after brain injury: mechanisms and principles. *Front Hum Neurosci, 7*, 887. doi:10.3389/fnhum.2013.00887

Park, H., & Poo, M. M. (2013). Neurotrophin regulation of neural circuit development and function. *Nat Rev Neurosci, 14*(1), 7-23. doi:10.1038/nrn3379

Paxinos, G., & Watson, C. (2007). *The rat brain in stereotaxic coordinates* (6th ed.). Amsterdam ; Boston ;: Academic Press/Elsevier.

Rocamora, N., Welker, E., Pascual, M., & Soriano, E. (1996). Upregulation of BDNF mRNA expression in the barrel cortex of adult mice after sensory stimulation. *J Neurosci, 16*(14), 4411-4419.

Schindelin, J., Arganda-Carreras, I., Frise, E., Kaynig, V., Longair, M., Pietzsch, T., . . . Cardona, A. (2012). Fiji: an open-source platform for biological-image analysis. *Nat Methods, 9*(7), 676-682. doi:10.1038/nmeth.2019

Song, W., Kerr, C. C., Lytton, W. W., & Francis, J. T. (2013). Cortical plasticity induced by spike-triggered microstimulation in primate somatosensory cortex. *PLoS One, 8*(3), e57453. doi:10.1371/journal.pone.0057453

Stroemer, R. P., Kent, T. A., & Hulsebosch, C. E. (1995). Neocortical neural sprouting, synaptogenesis, and behavioral recovery after neocortical infarction in rats. *Stroke, 26*(11), 2135-2144.

Strong, K., Mathers, C., & Bonita, R. (2007). Preventing stroke: saving lives around the world. *Lancet Neurol, 6*(2), 182-187. doi:10.1016/S1474-4422(07)70031-5

Uesaka, N., Hirai, S., Maruyama, T., Ruthazer, E. S., & Yamamoto, N. (2005). Activity dependence of cortical axon branch formation: a morphological and electrophysiological study using organotypic slice cultures. *J Neurosci, 25*(1), 1-9. doi:10.1523/JNEUROSCI.3855-04.2005

Uesaka, N., Ruthazer, E. S., & Yamamoto, N. (2006). The role of neural activity in cortical axon branching. *Neuroscientist, 12*(2), 102-106. doi:10.1177/1073858405281673